ACS OMEGA

Open Access

http://pubs.acs.org/journal/acsodf

Article

Lipopolysaccharide Detection with Glycan-Specific Lectins—a Nonspecific Binding Approach Applied to Surface Plasmon Resonance

Mathieu Lamarre and Denis Boudreau*

Cite This: ACS Omega 2025, 10, 15610−15620

Read Online

ACCESS | Metrics & More | Article Recommendations | Supporting Information

ABSTRACT: The detection and classification of lipopolysaccharides (LPS), pivotal constituents of Gram-negative bacteria, are fundamental to the progression of biosensing technologies in fields such as healthcare, environmental monitoring, and food safety. This study presents an innovative approach utilizing a panel of glycan-selective lectins in conjunction with surface plasmon resonance (SPR) providing a novel perspective on the evolution of biosensors within the context of the ongoing tension between the highly selective, one-probe-one-target methodology and the broader, resource-intensive approach that integrates complex and costly technological tools into the biosensing discipline. Guided by the principles of lean development, we employed a panel of lectins to construct multiprobe detection profiles, thereby facilitating the precise classification of LPS variants while minimizing both variability and resource expenditure. Advanced machine learning techniques were applied to optimize feature selection and enhance classification accuracy, demonstrating that a minimal set of four lectins sustains exceptional predictive performance. This synergy between traditional affinity techniques and data science enhances assay engineering efficiency, scalability, and integration into routine workflows, supporting frontline pathogen monitoring. This innovative approach holds promise for addressing global health challenges, providing more profound insights into biosensing methodologies, and expanding pathogen screening networks closer to the public and health safety management bodies.

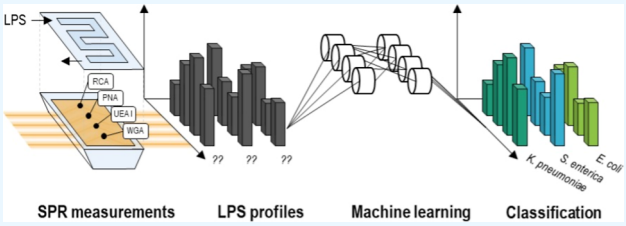

1. INTRODUCTION

Biosensors are crucial for detecting and distinguishing biomolecular species across vital scientific fields such as healthcare,[1−3] environmental monitoring,[3−7] and food safety.[8,9] In the evolving field of biosensor development, lean development principles have become increasingly important for optimizing assay efficiency and effectiveness. Lean principles emphasize the reduction of waste and the iterative enhancement of processes, which are crucial for the rapid and cost-effective development of bioanalytical methods.[10,11] The need for reliable metrics is paramount to enable decision-makers and researchers to monitor bioassay performance, control risks, and track processes over time. Furthermore, these metrics must be economically feasible and seamlessly integrable into routine workflows so frontline staff are able to utilize bioassays similarly to how they conduct daily monitoring of patients, environment, or market products.[12]

There is substantial interest in developing novel approaches to address these challenges, especially for the diagnostics of infectious diseases, a burden for global health causing millions of deaths every year.[13] In addition to the need for novel methods to detect bacterial pathogens, growing attention has been directed toward understanding the role of bacterial components such as lipopolysaccharides (LPS).[14−17] LPS are important outer membrane components of Gram-negative bacteria; they not only serve as markers of infection but also play a key role in triggering inflammatory responses in the human body.[18] They are particularly important in the context of gut health, where they contribute to complex disease mechanisms through bacterial interactions with the gastrointestinal tract.[19−21] Given the dual significance of LPS for both pathogen detection and their impact on human health, innovative biosensing technologies that can accurately and efficiently measure these components are essential. Such technologies must be capable of distinguishing between bacterial species based on LPS profiles while also providing insights into how these components influence broader health outcomes.

Advances in macromolecular engineering have led to the development of specific antibodies to target some of the main bacterial LPS.[22,23] However, despite these advances, batch-to-batch variability in biosynthesis and limited macromolecular stability after extraction processes can lead to significant

Received: January 28, 2025
Revised: March 31, 2025
Accepted: April 2, 2025
Published: April 7, 2025

https://doi.org/10.1021/acsomega.5c00867
ACS Omega 2025, 10, 15610−15620

variations in results and affect subsequent decision-making from these antibody-based methods.[24,25] Additionally, antibody probes often require constant redesigning due to target adaptation.[26,27] These challenges underscore the need for more robust, adaptable, and efficient techniques capable of offering real-time, precise, and high-throughput analysis of bacterial components like LPS.

The approach shown in this work aims to demonstrate that it is possible to dispense with highly specific molecular probes such as antibodies and to rely on a set of probes with lower specificity but, above all, variable specificity for different targets. We also want to show that the multiplicity of probe signals, insomuch as they differ between molecular targets, can be leveraged using statistical methods to discriminate between them with a single probe panel. We adopted a lean approach, using a panel of lectins covering a broad spectrum of glycan affinities, to iteratively guide the development of a novel method for detecting lipopolysaccharides (LPS). This approach leverages the intrinsic interactions between LPS glycans and glycan-selective lectins,[28−30] providing a more flexible and scalable solution for bacterial pathogen monitoring. This method uses surface plasmon resonance (SPR), a sensitive and label-free platform[31,32] able to accommodate multiple affinity probes and that has been proven effective as a rapid, specific, and noninvasive sensing technique for bacterial pathogen detection.[33−35] The democratization of computational techniques and advances in machine learning also empower the development of classification sensing approaches using panels of multiple probes. To this end, a machine learning-assisted decision scheme has been devised from existing models to improve the classification accuracy of our approach through feature selection modality.

Our approach aims to increase the synergy between traditional affinity binding techniques and modern data science tools. By guiding the development of classification methods through machine learning, we aim to achieve both simplicity and precision in bioassay design. This combination of lean principles, advanced affinity measurement techniques, and data-driven insights paves the way for more efficient and accurate biosensing tool development.

2. MATERIALS AND METHODS

2.1. Reagents. All chemicals were analytical reagent grade and used as received. Milli-Q water (18 mΩ) was used throughout this work. Afficoat, an antifouling peptide, was purchased from Affinité Instruments (Montréal, Canada). *N*-(3-(dimethylamino)propyl)-*N*′-ethylcarbodiimide hydrochloride (EDC), *N*-hydroxysuccinimide (NHS), sodium acetate, and ethanolamine were purchased from Sigma-Aldrich (Oakville, Canada). Phosphate buffer solution pH 7.4 (1X PBS) was purchased from Corning (Corning, US). Biotinylated lectins Concanavalin (ConA), *Glycine max* agglutinin (SBA), *Triticum vulgaris* agglutinin (WGA), *Dolichos biflorus* agglutinin (DBA), *Ulex europaeus* agglutinin (UEA I), *Ricinus communis* agglutinin (RCA), and Arachis hypogea agglutinin (PNA) were purchased from Vector Laboratories (Newark, US). Phenol extracted LPS from *E. coli* O55:B5 (CDC 1644-70), *E. coli* O111:B4 (private source), *K. pneumoniae* (ATCC 15830), *P. aeruginosa* (ATCC 27316), and *S. enterica* (ATCC 7823) were purchased from Sigma-Aldrich (Oakville, Canada).

2.2. Instrumentation. All SPR measurements were conducted using a 4-channel portable SPR (Model P4SPR, Affinité Instrument, Canada). The instrument's Dove prism enables wavelength-resolved plasmon shift measurements in real-time while minimizing the number of mechanical components. Briefly, the light from four coaligned and collimated LEDs is sent into the Dove prism supporting a thin gold layer deposited over a chromium adhesion layer. The beams emerging from the prism are directed through a polarizer (p or s polarization), collected by four optical fibers equipped with ball lenses (to maximize light collection efficiency), and transmitted to a compact grating spectrophotometer equipped with a CCD detector. The fluidic component, positioned on top of the prism, comprises four channels that can be probed separately or in sequence by controlling electrical power to the four LEDs. Various channel configurations are possible, such as a 3 + 1 configuration where one channel serves as a reference while the others are used as replicates, or a 4-channel configuration, where each individual channel can be functionalized with a different binding molecule.

2.3. Gold Deposition. Dove prisms (BK7 glass, Affinité Instrument, Canada) are first soaked in piranha solution (1:3 hydrogen peroxide and sulfuric acid), thoroughly rinsed with water, and then soaked in aqua regia (1:3 nitric acid and hydrochloric acid) to remove any remaining contaminants. After being thoroughly rinsed with water, prisms are soaked in soapy water, Milli-Q water, acetone, and isopropanol for 10 min each and finally dried with a stream of nitrogen gas. Prisms are placed in a physical vapor deposition (PVD) vacuum chamber, and 2 nm of chromium followed by 48 nm of gold is deposited. The layer thickness is measured with a quartz crystal microbalance (QCM).

2.4. Gold Surface Functionalization. The gold surface is first functionalized with a peptide designed to reduce nonspecific adhesion.[36] This 19-amino acid peptide carries a thiol function (3-mercaptopropionic acid) at the *N*-terminus, enabling the molecule to have a carboxylic acid function available for subsequent reactions. 4−5 droplets of a 100 μg/mL solution of Afficoat dissolved in DMF are deposited onto the gold surface and left to sit for 16 h before the prism is rinsed thoroughly with Milli-Q water and ethanol. The SPR shift is measured before and after this step to confirm proper prism functionalization [Figure S1 in Supporting Information (SI)]. Subsequent coupling reactions on the gold surface are carried out directly on the P4SPR using a 3 + 1-channel fluidic chamber connected to syringes, which enables the monitoring of surface mass transfer in real time. This chamber is equipped with two independent circuits, one for triplicate LPS detection and a second for monitoring surface integrity at each stage from functionalization to detection. The latter circuit is subject to the same conditions as the former, except for immobilization of molecular probes and injection of LPS, for which the buffers corresponding to these steps are injected. After a baseline is recorded for Milli-Q water, the activation of the carboxylic acid moiety with a 1:1 EDC (400 mM) and NHS (100 mM) mixture is carried out for 10 min, after which rinsing with acetate buffer (10 mM, pH 4.5) is performed to eliminate the unbound reagents. Injection of a 50 μM lectin solution in acetate buffer onto the freshly activated NHS-ester for 20 min allows for the formation of an amide bond. The SPR shift resulting from lectin immobilization is measured after an additional rinsing step with acetate buffer. Unreacted NHS-ester moieties are finally deactivated by injecting a 1 M solution of ethanolamine (pH 8.5) followed with phosphate buffer (Figure S2 in Supporting Information).

https://doi.org/10.1021/acsomega.5c00867
ACS Omega 2025, 10, 15610−15620

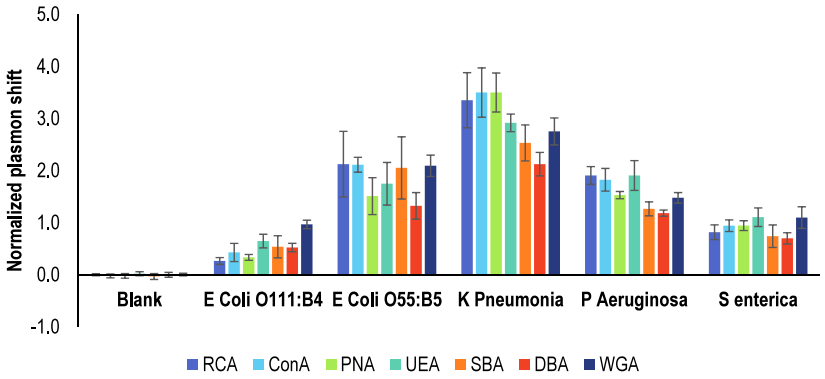

Figure 1. Lectin detection profiles. A total of 12 plasmon shift values, measured after 15 min of immobilization, were recorded for each lectin, with the average and standard deviation values represented by each band in the graph. Each lectin is used to create the LPS profiles for each bacterial species injected at 100 μg/mL, as well as a PBS buffer blank reference. The lectins chosen are Concanavalin (ConA), *Glycine max* agglutinin (SBA), *Triticum vulgaris* agglutinin (WGA), *Dolichos biflorus* agglutinin (DBA), *Ulex europaeus* agglutinin (UEA I), *Ricinus communis* agglutinin (RCA), and Arachis hypogea agglutinin (PNA). These lectins will be referred by their abbreviation for the next figures to avoid unnecessary length in the legend.

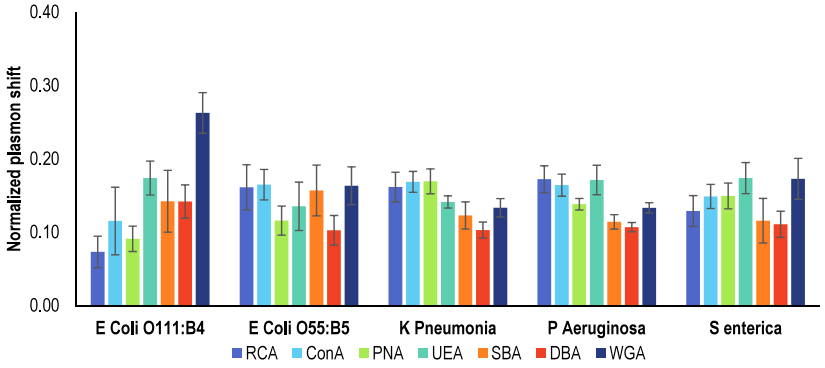

Figure 2. Normalized lectin detection profiles. Each of the 7-point profiles from the raw data set is subjected to L1 normalization. Each band represents the mean and standard deviation values for each lectin (n = 12), for both the bacterial species LPS and the blank.

2.5. LPS Detection. A solution of LPS diluted to 100 μg/mL with 1X PBS is injected into the fluidic chamber, and capture is carried out for 15 min, after which PBS is injected again. LPS affinity is assessed using a sensorgram to measure the SPR shift (Figure S3 in Supporting Information). A total of 12 sensorgrams are collected for each LPS and each molecular probe, allowing the generation of several profiles for each LPS mixture (Figure 1). These LPS come from five bacteria species that are known to cause severe infections in humans and exhibit variations in their lipopolysaccharide (LPS) structures, which influence host–pathogen interactions, virulence, and immune recognition.[37]

2.6. Machine Learning and Data Processing. The classification models used in this study are Random Forest (RF), k-Nearest Neighbors (kNN), and Support Vector Machine (SVM).[38−43] These models have been implemented using the scikit-learn Python library.[44] RF is an ensemble learning method that creates multiple decision trees during training and generates the majority class from the individual tree's predictions. On the other hand, the kNN is a simple, instance-based algorithm that classifies a data point based on the majority class among its k-nearest neighbors in the feature space. Finally, SVM is a powerful and versatile machine learning model capable of performing linear or nonlinear classification, regression, and outlier detection. It works by finding the hyperplane that best separates the classes in the feature space.

Prior to any computation, each raw profile is normalized by the integrated point values. Model selection and feature selection are conducted using a 10-time repeated cross-validation (3-fold) from which the mean accuracy and standard error are collected for optimization results.[45] Final metrics and confusion matrix are produced using a 10-times random data split with 3:1 split between training and validation subsets.[46] We evaluated the performance of optimized models using accuracy, recall, precision, and F1 score metrics. Accuracy represents the ratio of correctly classified observations relative to all observations, recall measures the ability to detect positive instances among actual cases, precision assesses the reliability of positive predictions and is expressed as the ratio of true positives to the total predicted positives, and the F1 score is the harmonic mean of precision and recall, providing a useful balance between these two metrics, particularly in contexts with imbalanced classes.[47]

3. RESULTS AND DISCUSSION

3.1. Detection of LPS. The detection of LPS by urface plasmon resonance using the 7 lectins enables the creation of detection profiles based on the differentiated specificity of said lectins for various glycans. These lectins present specific binding affinities for a broad set of glycan-rich residues (Table S1) found in O-glycan LPS moieties such as mannose (Man), *N*-acetylglucosamine (GluNAc), *N*-acetylgalactosamine (GalNAc), galactose (Gal), and fucose (Fuc). These 7-points

https://doi.org/10.1021/acsomega.5c00867
ACS Omega 2025, 10, 15610−15620

profiles have been obtained for the five LPS considered in this study, and the average and standard deviation values for the 12 replicates measured for each probe are summarized in Figure 1.

Each individual profile is normalized by the integrated point values, also known as L1 normalization, to reduce the variations that may occur due to variations in prism refractive index, efficiency of probe immobilization, or influence of the molecular mass of LPS on the SPR shift (Figure 2). This preprocessing is particularly important considering that the 7 points of the profile are independent, and their relative values are essential for distinguishing between different LPS species. No other preprocessing is applied to the data set, knowing that other scaling methods, e.g., standard scaling, min−max scaling, or absolute maximum scaling, assume that either each feature is normally distributed across the classes or that each value contributes equally to model classification, which, in this case, is not. On the contrary, the nonselective nature of lectins for a particular class of LPS raises the possibility that some lectins may be less influential than others in the classification performed by the machine learning model. Therefore, it is essential to avoid introducing bias by balancing the contribution of each lectin through scaling.

7-point profiles can be used to identify molecules just as one does with an infrared spectrum, where each feature (profile point or wavenumber value) is characteristic of one of the molecule's vibrational modes, and just as is the case with vibrational spectra, one can also use machine learning to enhance the classification capabilities of the profiles, albeit with a limited number of values (7 in this case) and the absence of interdependence between these values. In fact, each value on the profile is independent of its neighbor due to different times of acquisition and the complex binding affinity of lectins, unlike the values surrounding a point of an infrared spectrum, which vary interdependently as a function of molecular vibrations. It could be argued that if lectins are specific to the same glycan onto the LPS, there should be an interdependence between these points for the same LPS, but this would be true only if the lectin were exclusively specific to one glycan. However, it is well-known that lectins show different degrees of affinity for various glycans. For example, the detection sensitivity of RCA cannot be associated with the abundance of *N*-acetylgalactosamine alone since RCA also has a certain affinity for galactose and fucose residues.[48] To determine the degree of macromolecule glycosylation, one requires the use of multiple lectins to unravel these complex affinities, which is not the objective here.

3.2. Principal Component Analysis. Principal component analysis (PCA) was conducted on the 7-point profiles of LPS to discern underlying patterns and variations within the data set. The results are depicted in Figure 3, illustrating the scatter plot of PC1 against PC2 for each of the 5 types of LPS. The color-coded points on the graph emphasize the differences between the LPS types. PC1, explaining 58.2% of the total variance, and PC2, explaining 15.5%, collectively contribute to a significant portion of the data set's variability. Furthermore, a graph illustrating the cumulative explained variance of all principal components until reaching 100% variance elucidated the necessity of utilizing 5 to 6 PCs for dimension reduction, underscoring the complexity and multidimensionality of the data set (Figure 4).

We further investigated the importance of each feature within the profiles across all principal components. With this analysis, we aimed to identify the features driving the

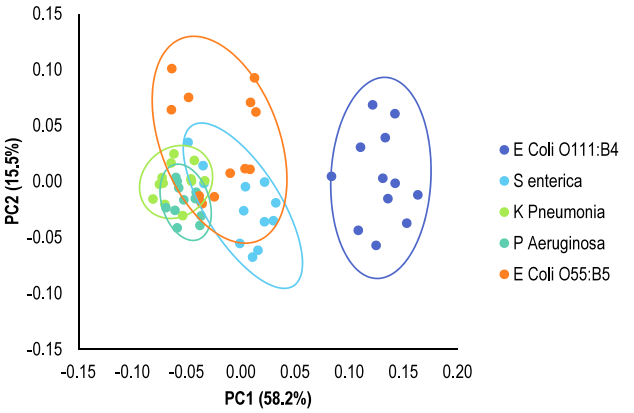

Figure 3. PC1 and PC2 graphical representation. PC1 explains 58.2% of the total variance in the data set, capturing the primary sources of variability between the samples. PC2 explains 15.5% of the variance, representing additional differences not captured by PC1. Each point on the plot corresponds to an individual sample, and the points are color-coded to represent different LPS from bacteria.

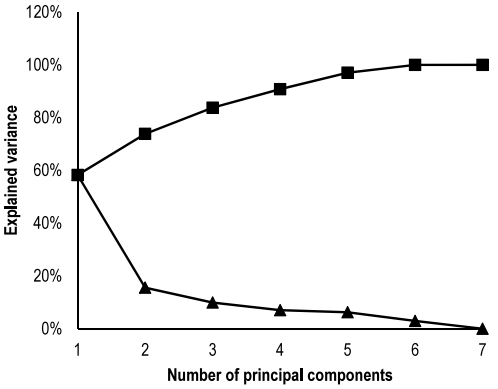

Figure 4. Proportion of variance of principal components. This graph displays the absolute explained variance for each of the 7 possible PCs (▲) and the cumulative explained variance for an increasing number of PCs (■).

dimensional reduction achieved by PCA. A graph was constructed to display the coefficients of each feature weighted by the explained variance of the corresponding principal component (Figure 5). Our findings revealed that features

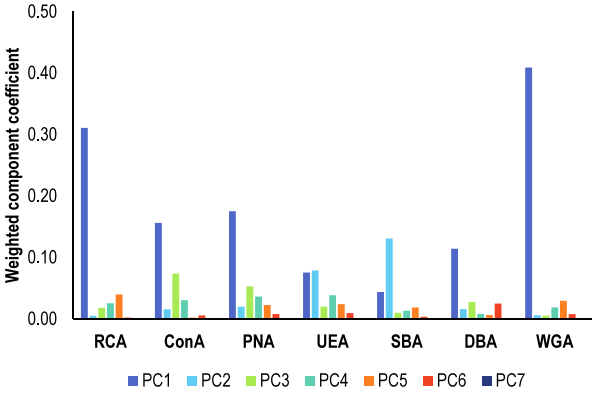

Figure 5. Weighted component coefficients. Principal component coefficients associated with each feature (plasmon shift values for each lectin) are multiplied by the absolute explained variance of the corresponding PC.

https://doi.org/10.1021/acsomega.5c00867
ACS Omega 2025, 10, 15610−15620

RCA, ConA, PNA, and WGA played a greater role in the dimension reduction process, as evidenced by their significant contributions to the explained variance across multiple principal components. Conversely, feature UEA, SBA, and DBA appeared to contribute less significantly to the variance captured by the PCAs.

While PCA provided valuable insights into the data structure, it was observed that PC1 and PC2 combined explained only approximately 70% of the total variance. This suggests that additional principal components may be required to effectively differentiate between the various LPS types. However, as PCA does not inherently focus on maximizing classes separability, relying solely on principal components may lead to suboptimal classification results, especially in cases where classes are not linearly separable. Consequently, the limitations of PCA in capturing complex patterns and class boundaries highlight the need for more sophisticated approaches. The use of machine learning techniques capable of learning complex, nonlinear relationships appears to be imperative for achieving a more granular classification of LPS types and enhancing overall accuracy.

3.3. Classification Model Selection. The first step in the machine learning classification process is the selection of a suitable classification model. For this purpose, model selection was performed using a 10-time repeated stratified 3-fold cross-validation on normalized profiles, with three models being evaluated: Random Forest (RF), k-Nearest Neighbors (kNN), and Support Vector Machine (SVM). The key hyperparameters of each model were optimized to maximize accuracy (Figures S4–S6 in Supporting Information). A significant difference in accuracy was observed among the models ($p > 0.05$) as shown in Figure 6, with SVM and RF slightly outperforming kNN. At this stage, no further optimization effort was pursued with kNN due to the lower performance of the model.

3.4. Feature Selection. The Random Forest model offers the ability to assess the relative importance of each lectin in the decision-making process. This importance is quantified by feature importance coefficients, which represent the contribution of each lectin in reducing the overall classification error in the RF model. These coefficients, presented in Figure 7, indicate how much each lectin improves the model's predictive accuracy by measuring the average decrease in node impurity when the feature is used to split the data across decision trees. However, it is important to note that these coefficients cannot be directly correlated with or interpreted as representing a higher level of abundance for a given variable. Instead, they solely reflect the variable's contribution to classification accuracy within the context of the RF model.

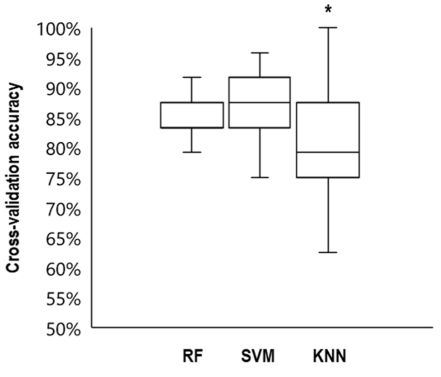

Figure 6. Cross-validation accuracy score. The three box plots represent the accuracies of the RF (trees = 100), SVM (kernel = RBF, C = 100), and kNN (neighbors = 3, weight = distance) models based on 10 repeated 3-fold cross-validation scores. The kNN model shows significantly lower accuracy than the RF and SVM models, with a p-value of less than 0.05. An asterisk indicates a distribution with a statistically significant difference in performance compared to the distribution without it.

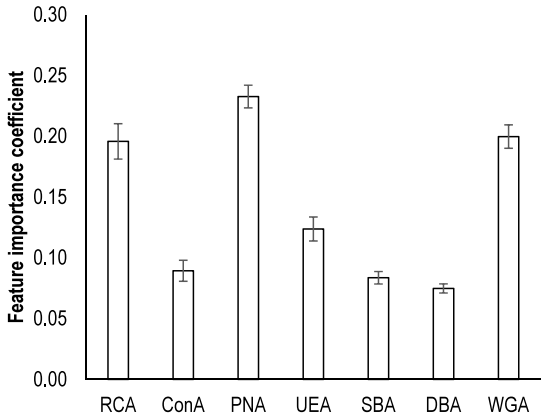

Figure 7. Feature importance coefficient. Each bar illustrates the mean importance coefficients for the 7 features associated with 7 lectins, calculated from 10 randomly selected train/test splits of the data set using a Random Forest model with 100 trees.

The results from 10 randomly selected-train/test splits of the data set show that RCA, PNA, and WGA exhibit higher importance, suggesting they play a pivotal role in the classification task, while the contributions of the other lectins are less pronounced. This could suggest greater variability in their abundance across the different LPS classes, whereas signals from the remaining lectins (ConA, SBA, DBA, and UEA) appear more consistent. Consequently, without further detailed information on the LPS composition, we cannot conclude whether glycans that bind to UEA, for example, are consistently absent or simply not detected on the analyzed LPS molecules.

Models like SVM and kNN do not provide feature importance metrics. The RF model's architecture, consisting of multiple decision trees, inherently allows for the calculation of these coefficients based on how often a feature is used and how effective it is in making splits. In contrast, SVM focuses on finding a hyperplane that best separates the data into classes, while kNN classifies based on the proximity of data points, and neither split data along features in a hierarchical manner. Therefore, determining the importance of individual features is not directly possible with these models.

The models were then trained and tested using all possible combinations of lectins, ranging from a single lectin to the full set of lectins in the original data set, to assess the classification capabilities for both models (RF and SVM) while overcoming SVM's inability to determine feature importance coefficients. The accuracy obtained with the best lectin combination found for each model is shown in Figure 8 (results for all lectin combinations are shown in Tables S2 and S3 in Supporting Information). Notably, a combination of three lectins yields performance comparable to the best results obtained with 4 or more lectins. Further analysis and the identified importance of each lectin in the model's decision-making process confirm that RCA, PNA, and WGA (or ConA, depending on the

https://doi.org/10.1021/acsomega.5c00867
ACS Omega 2025, 10, 15610−15620

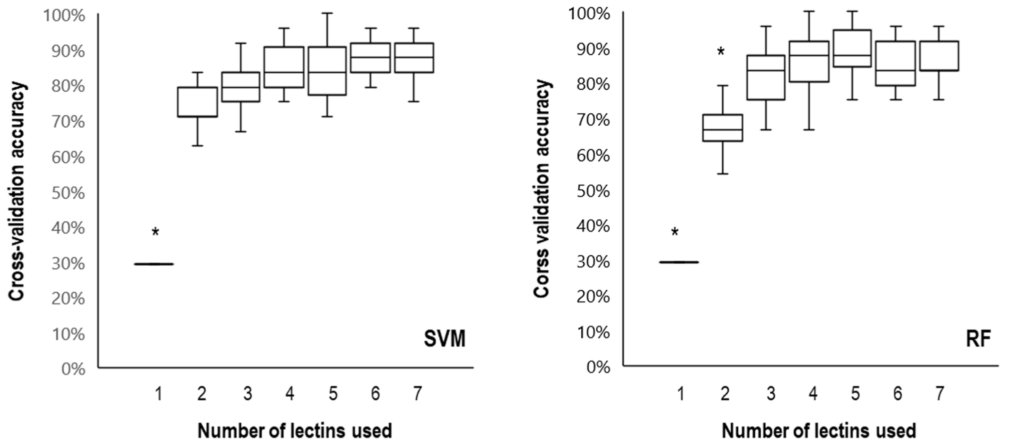

Figure 8. Feature reduction for RF and SVM machine learning models. The best-performing lectin set from the combination of increasing number of lectins (1 to 7, from left to right) is used in a 10 repeated 3-fold cross-validation to determine the accuracy for each model. Significant differences are assessed with a *t*-test ($p > 0.05$). An asterisk indicates a distribution with a statistically significant difference in performance compared to a distribution without it.

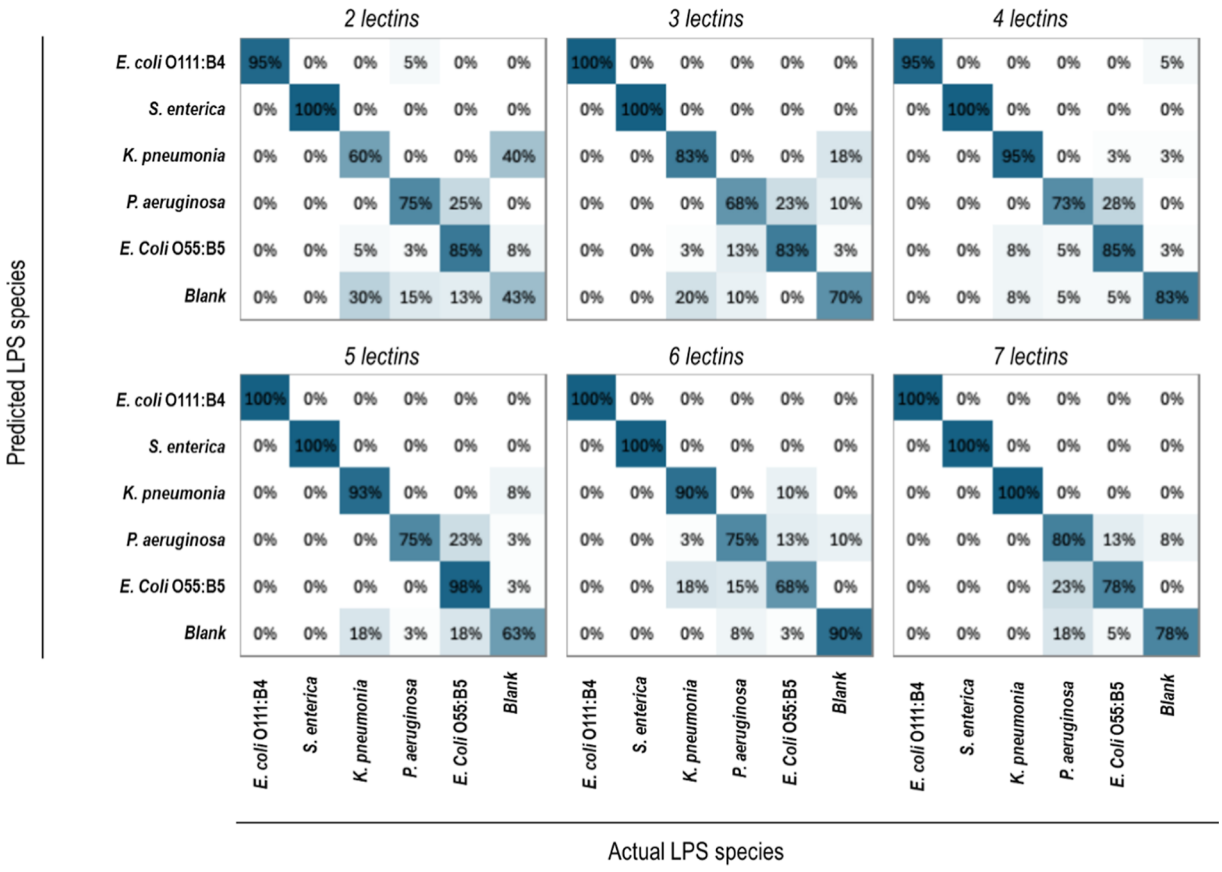

Figure 9. Support Vector Machine (SVM) confusion matrices for LPS classification with different profile lengths.

model) are consistently present in the most effective combinations. As shown in Figure 8, the performance gain is more pronounced for up to three lectins, providing either equivalent or superior accuracy compared to using all seven lectins.

While it may be argued that reducing the amount of data to decrease acquisition time or cost is unnecessary given that SPR imaging devices can perform multiple association measurements in parallel, this perspective primarily applies to centralized, method development laboratories. On the other hand, minimizing the number of features is essential in contexts where, for example, measurement space is limited such as in fluidic channels or when cost and complexity must be minimized such as disposable point-of-care testing.

3.5. Classification Performance. To assess the classification performance of both Support Vector Machine (SVM) and Random Forest (RF) models, confusion matrices (Figures 9 and 10) and several key metrics (accuracy, precision, recall, and F1 score) were calculated as a function of the numbers of lectins used in the profiles (Tables 1 and 2). The models were

https://doi.org/10.1021/acsomega.5c00867
ACS Omega 2025, 10, 15610−15620

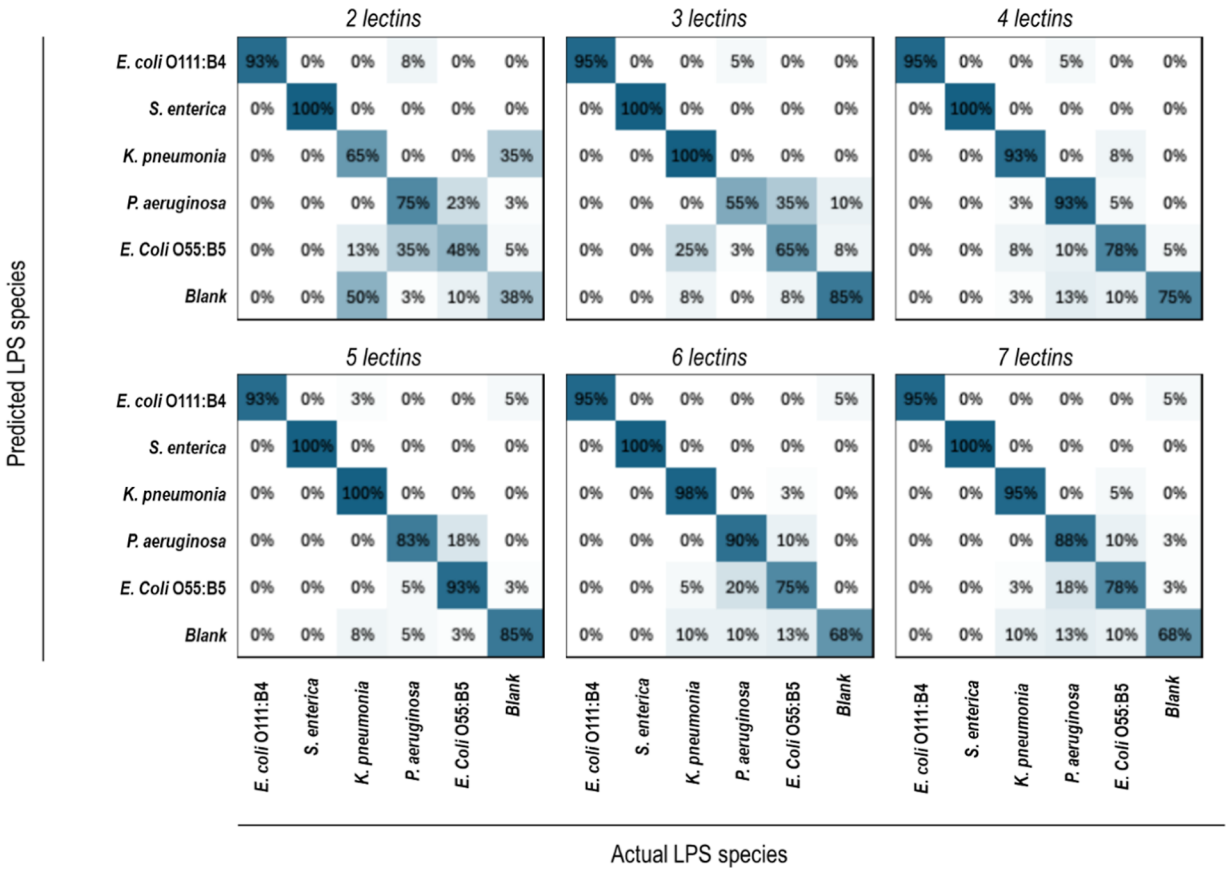

Figure 10. Random Forest (RF) confusion matrices for LPS classification with different profile lengths.

Table 1. Classification Report for Different Profile Lengths with the SVM Model

Nb. of lectins	lectins	accuracy		precision		recall		F1 score	
		mean	error	mean	error	mean	error	mean	error
2	PNA, WGA	76%	7%	77%	8%	76%	7%	75%	8%
3	ConA, PNA, WGA	84%	5%	86%	5%	84%	5%	83%	4%
4	RCA, PNA, UEA, WGA	88%	5%	91%	5%	88%	5%	88%	6%
5	RCA, ConA, PNA, UEA, WGA	88%	6%	91%	5%	88%	6%	87%	6%
6	RCA, ConA, PNA, UEA, SBA, WGA	87%	7%	90%	6%	87%	7%	86%	8%
7	RCA, ConA, PNA, UEA, SBA, DBA, WGA	89%	6%	92%	4%	89%	6%	89%	6%

Table 2. Classification Report for Different Profile Lengths with the RF Model

Nb. of lectin	lectins	accuracy		precision		recall		F1 score	
		mean	error	mean	error	mean	error	mean	error
2	PNA, WGA	70%	5%	71%	7%	70%	5%	68%	6%
3	RCA, PNA, WGA	83%	8%	87%	7%	83%	8%	82%	9%
4	RCA, PNA, UEA, WGA	89%	7%	91%	6%	89%	7%	89%	7%
5	RCA, PNA, SBA, DBA, WGA	92%	4%	93%	4%	92%	4%	92%	4%
6	RCA, PNA, UEA, SBA, DBA, WGA	88%	6%	90%	5%	88%	6%	87%	6%
7	RCA, ConA, PNA, UEA, SBA, DBA, WGA	87%	7%	89%	6%	87%	7%	86%	8%

trained to differentiate between five LPS samples and the blank, with profiles ranging from 7 lectins down to 2 lectins. This analysis, by providing insight into how accurately the models predict the correct classes and where classification errors occur, aimed to determine whether reducing the number of lectins would still provide acceptable classification performance, thereby minimizing the experimental time and resources required.

For both models, the diagonal cells of the matrices, representing correct classifications, contained the majority of the data when using 4 or more lectins, with off-diagonal elements accounting for no more than 13% of total predictions. This indicates that the models can accurately classify the LPS samples using profiles with up to 4 lectins, but as the number of lectins was reduced to 3 or fewer, classification errors increased noticeably. This was particularly true for *P. aeruginosa* and *E. coli* O55, which were frequently confused

https://doi.org/10.1021/acsomega.5c00867
ACS Omega 2025, 10, 15610−15620

with each other and with the blank. This increase in confusion suggests that these samples may share similar glycan structures, making them harder to distinguish with fewer lectins available to provide selective glycan binding.

The SVM model showed high performance with 7 lectins (RCA, ConA, PNA, UEA, SBA, DBA, WGA), achieving 89% accuracy (±6%), 92% precision (±4%), and a F1 score of 89% (±6%). Even as the number of lectins was reduced, the model maintained stable classification performance. Notably, profiles with 4 lectins (RCA, PNA, UEA, WGA) yielded an accuracy of 88% (±5%) and a F1 score of 88% (±6%), suggesting that four lectins are sufficient for reliable LPS classification. When the number of lectins was reduced to 3, the SVM model's performance was poorer, achieving 84% accuracy and a F1 score of 83%, while with 2 lectins, performance dropped further to 76% accuracy and a 75% F1 score. This marked decline suggests that profiles with fewer than 4 lectins lose too much discriminatory power, leading to significant misclassification.

The RF model exhibited a similar trend, with 7 lectins yielding 87% accuracy (±7%) and a F1 score of 86% (±8%). However, the best performance was observed with 5 lectins (RCA, PNA, SBA, DBA, WGA), achieving 92% accuracy (±4%) and a F1 score of 92% (±4%). This suggests that, for RF, a 5-lectin profile is optimal, providing the best balance between resource efficiency and classification performance. This also means that the exclusion of ConA and UEA can benefit the model's performance. With 6 lectins, the RF model maintained an accuracy of 88% (±6%) and a F1 score of 87% (±6%), while the 4-lectin profile also yielded a comparable performance (accuracy of 89% and F1 score of 89%). Like the SVM model, RF classification performance dropped significantly with 3 lectins (accuracy of 83%, F1 score of 82%) and 2 lectins (accuracy of 70%, F1 score of 68%). This suggests that RF, like SVM, requires at least 4 lectins to maintain performance compared to the full lectin set.

The analysis above shows that both the SVM and RF models perform comparably when profiles contain at least 4 lectins, allowing for effective classification of the five LPS samples and the blank. Reducing the number of lectins beyond this number leads to diminished classification performance, with both models experiencing significant drops in accuracy and F1 score when using 3 lectins or fewer. More precisely, a 4-lectin profile is the lower bound for maintaining classification performance in the case of the SVM model, while the RF model achieves optimal performance with 5 lectins. Both models demonstrate that profiles with 2 or 3 lectins result in substantial confusion, especially between *P. aeruginosa* and *E. coli* O55 as well as increased interference from the blank. This suggests that fewer lectins may fail to capture enough unique glycan interactions to reliably differentiate between these similar LPS molecules.

The lectin panel combined with the ML algorithms enhances specificity over traditional approaches, such as monoclonal antibody or limulus amoebocyte lysate (LAL) assays, by providing broader coverage of LPS variants. While an antibody is typically specific to a single LPS epitope and the LAL assay cannot differentiate between LPS variants, the lectin panel can recognize a wider range of LPS structures across different species based on the relative glycan content of the core and O-polysaccharide antigen that differ within and between bacterial species.[37] Additionally, the panel's adaptability allows it to be trained with LPS from emerging variants or new bacterial species, further expanding its recognition capabilities. This flexibility makes the lectin-based approach more versatile and effective for detecting diverse LPS structures compared to conventional antibody-based methods.

The present methodology could be implemented in a complex media, such as a culture medium, considering, on the one hand, that the immobilization of lectins is performed on an antifouling peptide (Affinicoat) that has demonstrated its ability to reduce nonspecific adhesion in matrices such as serum and blood plasma.[49] On the other hand, the fluidic system used with the P4SPR includes a reference channel that could be used to measure refractive index changes caused by the culture medium. Finally, an amplification method, such as secondary detection,[50] involving the subsequent injection—after LPS detection—of an anti-Lipid A polyclonal antibody solution, would provide a resonance wavelength shift specific to the presence of LPS considering they all display a lipid A region. These various strategies suggest that this detection method could be transferable to applications in complex environments after training the machine learning models.

4. CONCLUSION

This study aligns with the evolving landscape of biosensor development, where lean principles are essential for optimizing assay efficiency and effectiveness. Our exploration of surface plasmon resonance (SPR) in detecting and classifying lipopolysaccharides (LPS) exemplifies the application of these principles, emphasizing the reduction of waste through streamlined processes and the iterative enhancement of detection methodologies. By employing a panel of lectins, we established 7-point detection profiles for various LPS, facilitating robust classification while avoiding the pitfalls of batch-to-batch variability and the need for constant redesigning typical of antibody-based methods. This methodology increases the range of LPS that can be detected and identified with the same set of lectins and decrease the turnover time to add other LPS species in the training library compared to antibody engineering processes.

PCA analysis revealed significant patterns within our data, guiding the selection of key features that enhanced classification accuracy. Our findings demonstrated that specific lectins, especially RCA, PNA, and WGA, are pivotal in maintaining high classification performance, even as we optimized the number of lectins used in profiles.

Furthermore, the results of our machine learning-assisted approach underscore the synergy between traditional affinity techniques and modern data science. Both the Support Vector Machine (SVM) and Random Forest (RF) models exhibited strong capabilities in distinguishing between LPS types, particularly when utilizing profiles with four to seven lectin probes. Ultimately, this research contributes to the development of innovative biosensing technologies that not only accurately measure bacterial components but also introduce a procedure to reduce the number of necessary molecular probes. By leveraging a flexible and scalable approach to monitoring LPS, this work paves the way for more efficient and effective diagnostic tools, reinforcing the critical role of lean development principles in advancing the field of biosensors.

Despite the strong performance of the model, some limitations need to be addressed for broader applicability. First, the model's accuracy depends on the training data, making it unreliable for different sample conditions or concentrations. Expanding the data set with more diverse conditions would enhance robustness and generalizability.

https://doi.org/10.1021/acsomega.5c00867
ACS Omega 2025, 10, 15610−15620

Second, the model has not been tested on LPS mixtures. Addressing this would require either training on experimental mixtures or generating synthetic profiles. However, this shifts the problem to a regression task, requiring careful consideration of concentration effects on profiles. Finally, the model cannot detect unknown LPS and will always classify them into existing categories. Introducing an "unknown" class would help identify outliers and prevent misclassification. Future work will focus on these improvements to enhance the platform's flexibility and reliability in real-world applications.

■ ASSOCIATED CONTENT

Supporting Information

The Supporting Information is available free of charge at https://pubs.acs.org/doi/10.1021/acsomega.5c00867.

Additional data and methodological details supporting the main study, including experimental results, sensorgrams, and model optimization procedures, and a comprehensive view of the experimental procedures and computational analyses performed in the study (PDF)

■ AUTHOR INFORMATION

Corresponding Author

Denis Boudreau − *Department of Chemistry, Pavillon Alexandre-Vachon, 1045, avenue de la Médecine, Université Laval, Quebec City, Quebec G1 V0A6, Canada; Centre d'optique, photonique et lasers (COPL), Pavillon d'Optique-Photonique, 2375 rue de la Terrasse, Université Laval, Quebec City, Quebec G1 V0A6, Canada;* orcid.org/0000-0001-5152-2464; Email: denis.boudreau@chm.ulaval.ca

Author

Mathieu Lamarre − *Department of Chemistry, Pavillon Alexandre-Vachon, 1045, avenue de la Médecine, Université Laval, Quebec City, Quebec G1 V0A6, Canada; Centre d'optique, photonique et lasers (COPL), Pavillon d'Optique-Photonique, 2375 rue de la Terrasse, Université Laval, Quebec City, Quebec G1 V0A6, Canada*

Complete contact information is available at: https://pubs.acs.org/10.1021/acsomega.5c00867

Notes

The authors declare no competing financial interest.

■ ACKNOWLEDGMENTS

The authors thank M. Souleymane Toubou Bah (COPL thin film deposition platform) for assistance with metal PVD as well as lab members of Pr. Boudreau's research group for their valuable discussions and insights related to this work. M.L. thanks the NSERC-funded SMAART Program at U. Laval and le Fonds de recherche du Québec—Nature et technologies (FRQ-NT) for scholarships. This research was also supported by the Sentinel North program of Université Laval funded from the Canada First Research Excellence Fund.

■ REFERENCES

(1) Kim, E. R.; Joe, C.; Mitchell, R. J.; Gu, M. B. Biosensors for Healthcare: Current and Future Perspectives. *Trends Biotechnol.* **2023**, *41* (3), 374−395.

(2) Bhatia, D.; Paul, S.; Acharjee, T.; Ramachairy, S. S. Biosensors and Their Widespread Impact on Human Health. *Sens. Int.* **2024**, *5*, 100257.

(3) Gavrilaş, S.; Ursachi, C. Ş.; Perţa-Crişan, S.; Munteanu, F.-D. Recent Trends in Biosensors for Environmental Quality Monitoring. *Sensors* **2022**, *22* (4), 1513.

(4) Viegas, C. A. Chapter Four—Microbial Bioassays in Environmental Toxicity Testing. In *Advances in Applied Microbiology*; Gadd, G. M., Sariaslani, S., Eds.; Academic Press, 2021; Vol. *115*, pp 115−158..

(5) Lyne, T. B.; Bickham, J. W.; Lamb, T.; Gibbons, J. W. The Application of Bioassays in Risk Assessment of Environmental Pollution. *Risk Anal.* **1992**, *12* (3), 361−365.

(6) Popenda, A.; Wiśniowska, E.; Manuel, C. Biosensors in Environmental Analysis of Microplastics and Heavy Metal Compounds − A Review on Current Status and Challenges. *Desalin. Water Treat.* **2024**, *319*, 100456.

(7) Huang, C.-W.; Lin, C.; Nguyen, M. K.; Hussain, A.; Bui, X.-T.; Ngo, H. H. A Review of Biosensor for Environmental Monitoring: Principle, Application, and Corresponding Achievement of Sustainable Development Goals. *Bioengineered* **2023**, *14* (1), 58−80.

(8) Meliana, C.; Liu, J.; Show, P. L.; Low, S. S. Biosensor in Smart Food Traceability System for Food Safety and Security. *Bioengineered* **2024**, *15* (1), 2310908.

(9) Zhang, J.; Huang, H.; Song, G.; Huang, K.; Luo, Y.; Liu, Q.; He, X.; Cheng, N. Intelligent Biosensing Strategies for Rapid Detection in Food Safety: A Review. *Biosens. Bioelectron.* **2022**, *202*, 114003.

(10) Cummings, J.; Raynaud, F.; Jones, L.; Sugar, R.; Dive, C. Fit-for-Purpose Biomarker Method Validation for Application in Clinical Trials of Anticancer Drugs. *Br. J. Cancer* **2010**, *103* (9), 1313−1317.

(11) Pessôa, M. V. P. *Planning to Lean Product Development: A Mindset Change*; PMI® Global Congress 2007: Cancun, 2007.

(12) Srinivasan, B.; Tung, S. Development and Applications of Portable Biosensors. *SLAS Technol.* **2015**, *20* (4), 365−389.

(13) Ikuta, K. S.; Swetschinski, L. R.; Robles Aguilar, G.; Sharara, F.; Mestrovic, T.; Gray, A. P.; Davis Weaver, N.; Wool, E. E.; Han, C.; Gershberg Hayoon, A.; Aali, A.; Abate, S. M.; Abbasi-Kangevari, M.; Abbasi-Kangevari, Z.; Abd-Elsalam, S.; Abebe, G.; Abedi, A.; Abhari, A. P.; Abidi, H.; Aboagye, R. G.; Absalan, A.; Abubaker Ali, H.; Acuna, J. M.; Adane, T. D.; Addo, I. Y.; Adegboye, O. A.; Adnan, M.; Adnani, Q. E. S.; Afzal, M. S.; Afzal, S.; Aghdam, Z. B.; Ahinkorah, B. O.; Ahmad, A.; Ahmad, A. R.; Ahmad, R.; Ahmad, S.; Ahmad, S.; Ahmadi, S.; Ahmed, A.; Ahmed, H.; Ahmed, J. Q.; Ahmed Rashid, T.; Ajami, M.; Aji, B.; Akbarzadeh-Khiavi, M.; Akunna, C. J.; Al Hamad, H.; Alahdab, F.; Al-Aly, Z.; Aldeyab, M. A.; Aleman, A. V.; Alhalaiqa, F. A. N.; Alhassan, R. K.; Ali, B. A.; Ali, L.; Ali, S. S.; Alimohamadi, Y.; Alipour, V.; Alizadeh, A.; Aljunid, S. M.; Allel, K.; Almustanyir, S.; Ameyaw, E. K.; Amit, A. M. L.; Anandavelane, N.; Ancuceanu, R.; Andrei, C. L.; Andrei, T.; Anggraini, D.; Ansar, A.; Anyasodor, A. E.; Arabloo, J.; Aravkin, A. Y.; Areda, D.; Aripov, T.; Artamonov, A. A.; Arulappan, J.; Aruleba, R. T.; Asaduzzaman, M.; Ashraf, T.; Athari, S. S.; Atlaw, D.; Attia, S.; Ausloos, M.; Awoke, T.; Ayala Quintanilla, B. P.; Ayana, T. M.; Azadnajafabad, S.; Azari Jafari, A.; B, D. B.; Badar, M.; Badiye, A. D.; Baghcheghi, N.; Bagherieh, S.; Baig, A. A.; Banerjee, I.; Barac, A.; Bardhan, M.; Barone-Adesi, F.; Barqawi, H. J.; Barrow, A.; Baskaran, P.; Basu, S.; Batiha, A.-M. M.; Bedi, N.; Belete, M. A.; Belgaumi, U. I.; Bender, R. G.; Bhandari, B.; Bhandari, D.; Bhardwaj, P.; Bhaskar, S.; Bhattacharyya, K.; Bhattarai, S.; Bitaraf, S.; Buonsenso, D.; Butt, Z. A.; Caetano dos Santos, F. L.; Cai, J.; Calina, D.; Camargos, P.; Cámera, L. A.; Cárdenas, R.; Cevik, M.; Chadwick, J.; Charan, J.; Chaurasia, A.; Ching, P. R.; Choudhari, S. G.; Chowdhury, E. K.; Chowdhury, F. R.; Chu, D.-T.; Chukwu, I. S.; Dadras, O.; Dagnaw, F. T.; Dai, X.; Das, S.; Dastiridou, A.; Debela, S. A.; Demisse, F. W.; Demissie, S.; Dereje, D.; Derese, M.; Desai, H. D.; Dessalegn, F. N.; Dessalegni, S. A. A.; Desye, B.; Dhaduk, K.; Dhimal, M.; Dhingra, S.; Diao, N.; Diaz, D.; Djalalinia, S.; Dodangeh, M.; Dongarwar, D.; Dora, B. T.; Dorostkar, F.; Dsouza, H. L.; Dubljanin, E.; Dunachie, S. J.; Durojaiye, O. C.; Edinur, H. A.; Ejigu, H. B.; Ekholuenetale, M.; Ekundayo, T. C.; El-Abid, H.; Elhadi, M.;

Elmonem, M. A.; Emami, A.; Engelbert Bain, L.; Enyew, D. B.; Erkhembayar, R.; Eshrati, B.; Etaee, F.; Fagbamigbe, A. F.; Falahi, S.; Fallahzadeh, A.; Faraon, E. J. A.; Fatehizadeh, A.; Fekadu, G.; Fernandes, J. C.; Ferrari, A.; Fetensa, G.; Filip, I.; Fischer, F.; Foroutan, M.; Gaal, P. A.; Gadanya, M. A.; Gaidhane, A. M.; Ganesan, B.; Gebrehiwot, M.; Ghanbari, R.; Ghasemi Nour, M.; Ghashghaee, A.; Gholamrezanezhad, A.; Gholizadeh, A.; Golechha, M.; Goleij, P.; Golinelli, D.; Goodridge, A.; Gunawardane, D. A.; Guo, Y.; Gupta, R. D.; Gupta, S.; Gupta, V. B.; Gupta, V. K.; Guta, A.; Habibzadeh, P.; Haddadi Avval, A.; Halwani, R.; Hanif, A.; Hannan, Md. A.; Harapan, H.; Hassan, S.; Hassankhani, H.; Hayat, K.; Heibati, B.; Heidari, G.; Heidari, M.; Heidari-Soureshjani, R.; Herteliu, C.; Heyi, D. Z.; Hezam, K.; Hoogar, P.; Horita, N.; Hossain, M. M.; Hosseinzadeh, M.; Hostiuc, M.; Hostiuc, S.; Hoveidamanesh, S.; Huang, J.; Hussain, S.; Hussein, N. R.; Ibitoye, S. E.; Ilesanmi, O. S.; Ilic, I. M.; Ilic, M. D.; Imam, M. T.; Immurana, M.; Inbaraj, L. R.; Iradukunda, A.; Ismail, N. E.; Iwu, C. C. D.; Iwu, C. J.; J, L. M.; Jakovljevic, M.; Jamshidi, E.; Javaheri, T.; Javanmardi, F.; Javidnia, J.; Jayapal, S. K.; Jayarajah, U.; Jebai, R.; Jha, R. P.; Joo, T.; Joseph, N.; Joukar, F.; Jozwiak, J. J.; Kacimi, S. E. O.; Kadashetti, V.; Kalankesh, L. R.; Kalhor, R.; Kamal, V. K.; Kandel, H.; Kapoor, N.; Karkhah, S.; Kassa, B. G.; Kassebaum, N. J.; Katoto, P. D.; Keykhaei, M.; Khajuria, H.; Khan, A.; Khan, I. A.; Khan, M.; Khan, M. N.; Khan, M. A.; Khatatbeh, M. M.; Khater, M. M.; Khayat Kashani, H. R.; Khubchandani, J.; Kim, H.; Kim, M. S.; Kimokoti, R. W.; Kissoon, N.; Kochhar, S.; Kompani, F.; Kosen, S.; Koul, P. A.; Koulmane Laxminarayana, S. L.; Krapp Lopez, F.; Krishan, K.; Krishnamoorthy, V.; Kulkarni, V.; Kumar, N.; Kurmi, O. P.; Kuttikkattu, A.; Kyu, H. H.; Lal, D. K.; Lám, J.; Landires, I.; Lasrado, S.; Lee, S.; Lenzi, J.; Lewycka, S.; Li, S.; Lim, S. S.; Liu, W.; Lodha, R.; Loftus, M. J.; Lohiya, A.; Lorenzovici, L.; Lotfi, M.; Mahmoodpoor, A.; Mahmoud, M. A.; Mahmoudi, R.; Majeed, A.; Majidpoor, J.; Makki, A.; Mamo, G. A.; Manla, Y.; Martorell, M.; Matei, C. N.; McManigal, B.; Mehrabi Nasab, E.; Mehrotra, R.; Melese, A.; Mendoza-Cano, O.; Menezes, R. G.; Mentis, A.-F. A.; Micha, G.; Michalek, I. M.; Micheletti Gomide Nogueira de Sá, A. C.; Milevska Kostova, N.; Mir, S. A.; Mirghafourvand, M.; Mirmoeeni, S.; Mirrakhimov, E. M.; Mirza-Aghazadeh-Attari, M.; Misganaw, A. S.; Misganaw, A.; Misra, S.; Mohammadi, E.; Mohammadi, M.; Mohammadian-Hafshejani, A.; Mohammed, S.; Mohan, S.; Mohseni, M.; Mokdad, A. H.; Momtazmanesh, S.; Monasta, L.; Moore, C. E.; Moradi, M.; Moradi Sarabi, M.; Morrison, S. D.; Motaghinejad, M.; Mousavi Isfahani, H.; Mousavi Khaneghah, A.; Mousavi-Aghdas, S. A.; Mubarik, S.; Mulita, F.; Mulu, G. B. B.; Munro, S. B.; Muthupandian, S.; Nair, T. S.; Naqvi, A. A.; Narang, H.; Natto, Z. S.; Naveed, M.; Nayak, B. P.; Naz, S.; Negoi, I.; Nejadghaderi, S. A.; Neupane Kandel, S.; Ngwa, C. H.; Niazi, R. K.; Nogueira de Sá, A. T.; Noroozi, N.; Nouraei, H.; Nowroozi, A.; Nuñez-Samudio, V.; Nutor, J. J.; Nzoputam, C. I.; Nzoputam, O. J.; Oancea, B.; Obaidur, R. M.; Ojha, V. A.; Okekunle, A. P.; Okonji, O. C.; Olagunju, A. T.; Olusanya, B. O.; Omar Bali, A.; Omer, E.; Otstavnov, N.; Oumer, B.; P A, M.; Padubidri, J. R.; Pakshir, K.; Palicz, T.; Pana, A.; Pardhan, S.; Paredes, J. L.; Parekh, U.; Park, E.-C.; Park, S.; Pathak, A.; Paudel, R.; Paudel, U.; Pawar, S.; Pazoki Toroudi, H.; Peng, M.; Pensato, U.; Pepito, V. C. F.; Pereira, M.; Peres, M. F. P.; Perico, N.; Petcu, I.-R.; Piracha, Z. Z.; Podder, I.; Pokhrel, N.; Poluru, R.; Postma, M. J.; Pourtaheri, N.; Prashant, A.; Qattea, I.; Rabiee, M.; Rabiee, N.; Radfar, A.; Raeghi, S.; Rafiei, S.; Raghav, P. R.; Rahbarnia, L.; Rahimi-Movaghar, V.; Rahman, M.; Rahman, M. A.; Rahmani, A. M.; Rahmanian, V.; Ram, P.; Ranjha, M. M. A. N.; Rao, S. J.; Rashidi, M.-M.; Rasul, A.; Ratan, Z. A.; Rawaf, S.; Rawassizadeh, R.; Razeghinia, M. S.; Redwan, E. M. M.; Regasa, M. T.; Remuzzi, G.; Reta, M. A.; Rezaei, N.; Rezapour, A.; Riad, A.; Ripon, R. K.; Rudd, K. E.; Saddik, B.; Sadeghian, S.; Saeed, U.; Safaei, M.; Safary, A.; Safi, S. Z.; Sahebazzamani, M.; Sahebkar, A.; Sahoo, H.; Salahi, S.; Salahi, S.; Salari, H.; Salehi, S.; Samadi Kafil, H.; Samy, A. M.; Sanadgol, N.; Sankararaman, S.; Sanmarchi, F.; Sathian, B.; Sawhney, M.; Saya, G. K.; Senthilkumaran, S.; Seylani, A.; Shah, P. A.; Shaikh, M. A.; Shaker, E.; Shakhmardanov, M. Z.; Sharew, M. M.; Sharifi-Razavi, A.; Sharma, P.; Sheikhi, R. A.; Sheikhy, A.; Shetty, P. H.; Shigematsu, M.; Shin, J. Il.; Shirzad-Aski, H.; Shivakumar, K. M.; Shobeiri, P.; Shorofi, S. A.; Shrestha, S.; Sibhat, M. M.; Sidemo, N. B.; Sikder, M. K.; Silva, L. M. L. R.; Singh, J. A.; Singh, P.; Singh, S.; Siraj, M. S.; Siwal, S. S.; Skryabin, V. Y.; Skryabina, A. A.; Socea, B.; Solomon, D. D.; Song, Y.; Sreeramareddy, C. T.; Suleman, M.; Suliankatchi Abdulkader, R.; Sultana, S.; Szócska, M.; Tabatabaeizadeh, S.-A.; Tabish, M.; Taheri, M.; Taki, E.; Tan, K.-K.; Tandukar, S.; Tat, N. Y.; Tat, V. Y.; Tefera, B. N.; Tefera, Y. M.; Temesgen, G.; Temsah, M.-H.; Tharwat, S.; Thiyagarajan, A.; Tleyjeh, I. I.; Troeger, C. E.; Umapathi, K. K.; Upadhyay, E.; Valadan Tahbaz, S.; Valdez, P. R.; Van den Eynde, J.; van Doorn, H. R.; Vaziri, S.; Verras, G.-I.; Viswanathan, H.; Vo, B.; Waris, A.; Wassie, G. T.; Wickramasinghe, N. D.; Yaghoubi, S.; Yahya, G. A. T. Y.; Yahyazadeh Jabbari, S. H.; Yigit, A.; Yiğit, V.; Yon, D. K.; Yonemoto, N.; Zahir, M.; Zaman, B. A.; Zaman, S. B.; Zangiabadian, M.; Zare, I.; Zastrozhin, M. S.; Zhang, Z.-J.; Zheng, P.; Zhong, C.; Zoladl, M.; Zumla, A.; Hay, S. I.; Dolecek, C.; Sartorius, B.; Murray, C. J. L.; Naghavi, M. Global Mortality Associated with 33 Bacterial Pathogens in 2019: A Systematic Analysis for the Global Burden of Disease Study 2019. *Lancet* **2022**, *400* (10369), 2221−2248.

(14) Fan, Y.; Pedersen, O. Gut Microbiota in Human Metabolic Health and Disease. *Nat. Rev. Microbiol.* **2021**, *19*, 55−71.

(15) Abautret-Daly, A.; Dempsey, E.; Parra-Blanco, A.; Medina, C.; Harkin, A. Gut−Brain Actions Underlying Comorbid Anxiety and Depression Associated with Inflammatory Bowel Disease. *Acta Neuropsychiatr.* **2018**, *30* (5), 275−296.

(16) Humbel, F.; Rieder, J. H.; Franc, Y.; Juillerat, P.; Scharl, M.; Misselwitz, B.; Schreiner, P.; Begré, S.; Rogler, G.; von Känel, R.; Yilmaz, B.; Biedermann, L. Association of Alterations in Intestinal Microbiota With Impaired Psychological Function in Patients With Inflammatory Bowel Diseases in Remission. *Clin. Gastroenterol. Hepatol.* **2020**, *18* (9), 2019−2029.

(17) Tang, Z.-Z.; Chen, G.; Hong, Q.; Huang, S.; Smith, H. M.; Shah, R. D.; Scholz, M.; Ferguson, J. F. Multi-Omic Analysis of the Microbiome and Metabolome in Healthy Subjects Reveals Microbiome-Dependent Relationships Between Diet and Metabolites. *Front. Genet.* **2019**, *10* (MAY), 454.

(18) Cani, P. D.; Amar, J.; Iglesias, M. A.; Poggi, M.; Knauf, C.; Bastelica, D.; Neyrinck, A. M.; Fava, F.; Tuohy, K. M.; Chabo, C.; Waget, A.; Delmee, E.; Cousin, B.; Sulpice, T.; Chamontin, B.; Ferrieres, J.; Tanti, J.-F.; Gibson, G. R.; Casteilla, L.; Delzenne, N. M.; Alessi, M. C.; Burcelin, R. Metabolic Endotoxemia Initiates Obesity and Insulin Resistance. *Diabetes* **2007**, *56* (7), 1761−1772.

(19) Abreu, M. T. Toll-like Receptor Signalling in the Intestinal Epithelium: How Bacterial Recognition Shapes Intestinal Function. *Nat. Rev. Immunol.* **2010**, *10* (2), 131−144.

(20) Chen, M. X.; Wang, S.-Y.; Kuo, C.-H.; Tsai, I.-L. Metabolome Analysis for Investigating Host-Gut Microbiota Interactions. *J. Formosan Med. Assoc.* **2019**, *118*, S10−S22.

(21) Moludi, J.; Maleki, V.; Jafari-Vayghyan, H.; Vaghef-Mehrabany, E.; Alizadeh, M. Metabolic Endotoxemia and Cardiovascular Disease: A Systematic Review about Potential Roles of Prebiotics and Probiotics. *Clin. Exp. Pharmacol. Physiol.* **2020**, *47* (6), 927−939.

(22) Vacca, F.; Sala, C.; Rappuoli, R. Monoclonal Antibodies for Bacterial Pathogens: Mechanisms of Action and Engineering Approaches for Enhanced Effector Functions. *Biomedicines* **2022**, *10* (9), 2126.

(23) Soliman, C.; Pier, G. B.; Ramsland, P. A. Antibody Recognition of Bacterial Surfaces and Extracellular Polysaccharides. *Curr. Opin. Struct. Biol.* **2020**, *62*, 48−55.

(24) Luo, Y.; Pehrsson, M.; Langholm, L.; Karsdal, M.; Bay-Jensen, A.-C.; Sun, S. Lot-to-Lot Variance in Immunoassays—Causes, Consequences, and Solutions. *Diagnostics* **2023**, *13* (11), 1835.

(25) Ma, H.; Ó'Fágáin, C.; O'Kennedy, R. Antibody Stability: A Key to Performance - Analysis, Influences and Improvement. *Biochimie* **2020**, *177*, 213−225.

(26) Byrne, B.; Stack, E.; Gilmartin, N.; O'Kennedy, R. Antibody-Based Sensors: Principles, Problems and Potential for Detection of Pathogens and Associated Toxins. *Sensors* **2009**, *9* (6), 4407−4445.

https://doi.org/10.1021/acsomega.5c00867
ACS Omega 2025, 10, 15610−15620

(27) Dunlap, T.; Cao, Y. Physiological Considerations for Modeling in Vivo Antibody-Target Interactions. *Front. Pharmacol* **2022**, *13*, 856961.
(28) Mattox, D. E.; Bailey-Kellogg, C. Comprehensive Analysis of Lectin-Glycan Interactions Reveals Determinants of Lectin Specificity. *PLoS Comput. Biol.* **2021**, *17* (10), No. e1009470.
(29) Hassan, S.-U.; Donia, A.; Sial, U.; Zhang, X.; Bokhari, H. Glycoprotein- and Lectin-Based Approaches for Detection of Pathogens. *Pathogens* **2020**, *9* (9), 694.
(30) Tsaneva, M.; Van Damme, E. J. M. 130 Years of Plant Lectin Research. *Glycoconjugate J.* **2020**, *37* (5), 533−551.
(31) Bolduc, O. R.; Live, L. S.; Masson, J.-F. High-Resolution Surface Plasmon Resonance Sensors Based on a Dove Prism. *Talanta* **2009**, *77* (5), 1680−1687.
(32) Qu, J. H.; Dillen, A.; Saeys, W.; Lammertyn, J.; Spasic, D. Advancements in SPR Biosensing Technology: An Overview of Recent Trends in Smart Layers Design, Multiplexing Concepts, Continuous Monitoring and in Vivo Sensing. *Anal. Chim. Acta* **2020**, *1104*, 10−27.
(33) Thawany, P.; Tiwari, U. K.; Deep, A. Surface Plasmon Resonance (SPR)-Based Nanosensors for the Detection of Pathogenic Bacteria. In *Nanosensors for Point-of-Care Diagnostics of Pathogenic Bacteria*; Acharya, A., Singhal, N. K., Eds.; Springer Nature Singapore: Singapore, 2023; pp 41−57..
(34) Brogioni, B.; Berti, F. Surface Plasmon Resonance for the Characterization of Bacterial Polysaccharide Antigens: A Review. *Medchemcomm* **2014**, *5* (8), 1058−1066.
(35) Park, J.-H.; Cho, Y.-W.; Kim, T.-H. Recent Advances in Surface Plasmon Resonance Sensors for Sensitive Optical Detection of Pathogens. *Biosensors* **2022**, *12* (3), 180.
(36) Bolduc, O. R.; Masson, J. F. Monolayers of 3-Mercaptopropyl-Amino Acid to Reduce the Nonspecific Adsorption of Serum Proteins on the Surface of Biosensors. *Langmuir* **2008**, *24* (20), 12085−12091.
(37) Mohebbanaaz; Rajani Kumari, L. V.; Padma Sai, Y. Classification of Arrhythmia Beats Using Optimized K-Nearest Neighbor Classifier. *Intell. Syst.* **2021**, *185*, 349−359.
(38) Guido, R.; Groccia, M. C.; Conforti, D. A Hyper-Parameter Tuning Approach for Cost-Sensitive Support Vector Machine Classifiers. *Soft Comput.* **2023**, *27* (18), 12863−12881.
(39) Dioşan, L.; Rogozan, A.; Pecuchet, J.-P. Improving Classification Performance of Support Vector Machine by Genetically Optimising Kernel Shape and Hyper-Parameters. *Appl. Intell.* **2012**, *36* (2), 280−294.
(40) Zhu, N.; Zhu, C.; Zhou, L.; Zhu, Y.; Zhang, X. Optimization of the Random Forest Hyperparameters for Power Industrial Control Systems Intrusion Detection Using an Improved Grid Search Algorithm. *Appl. Sci.* **2022**, *12* (20), 10456.
(41) Bonaccorso, G. *Machine Learning Algorithms*, 2nd ed.; Packt Publishing, 2018.
(42) Sarker, I. H. Machine Learning: Algorithms, Real-World Applications and Research Directions. *SN Comput. Sci.* **2021**, *2* (3), 160.
(43) Pedregosa, F.; Varoquaux, G.; Gramfort, A.; Michel, V.; Thirion, B.; Grisel, O.; Blondel, M.; Prettenhofer, P.; Weiss, R.; Dubourg, V.; Vanderplas, J.; Passos, A.; Cournapeau, D.; Brucher, M.; Perrot, M.; Duchesnay, E.ˊ. Scikit-Learn: Machine Learning in Python. *J. Mach. Learn. Res.* **2011**, *12*, 2825−2830.
(44) Wong, T.-T. Performance Evaluation of Classification Algorithms by K-Fold and Leave-One-out Cross Validation. *Pattern Recognit.* **2015**, *48* (9), 2839−2846.
(45) Xu, Y.; Goodacre, R. On Splitting Training and Validation Set: A Comparative Study of Cross-Validation, Bootstrap and Systematic Sampling for Estimating the Generalization Performance of Supervised Learning. *J. Anal Test* **2018**, *2* (3), 249−262.
(46) Sokolova, M.; Lapalme, G. A Systematic Analysis of Performance Measures for Classification Tasks. *Inf. Process. Manage.* **2009**, *45* (4), 427−437.
(47) Zhang, L.; Luo, S.; Zhang, B. The Use of Lectin Microarray for Assessing Glycosylation of Therapeutic Proteins. *MAbs* **2016**, *8* (3), 524−535.
(48) Stromberg, L. R.; Mendez, H. M.; Mukundan, H. Detection Methods for Lipopolysaccharides: Past and Present. *IntechOpen* **2017**, *24*..
(49) Bolduc, O. R.; Pelletier, J. N.; Masson, J.-F. SPR Biosensing in Crude Serum Using Ultralow Fouling Binary Patterned Peptide SAM. *Anal. Chem.* **2010**, *82* (9), 3699−3706.
(50) Hong, X.; Hall, E. A. H. Contribution of Gold Nanoparticles to the Signal Amplification in Surface Plasmon Resonance. *Analyst* **2012**, *137* (20), 4712−4719.

https://doi.org/10.1021/acsomega.5c00867
ACS Omega 2025, 10, 15610−15620